

# NEW VECTORIAL FINITE-ELEMENT BPM FOR OPTICAL ANISOTROPIC WAVEGUIDES

J. P. da Silva and H. E. Hernández-Figueroa

Universidade Estadual de Campinas  
Faculdade de Engenharia Elétrica e de Computação, Departamento de Microondas e Óptica  
P. O. Box 6101, 13083-970, Campinas-SP, Brazil

**Abstract** - An efficient finite-element vector beam propagation formulation for dielectric media with transverse anisotropy is thoroughly presented. This formulation is expressed in terms of the magnetic field's transverse components and includes perfectly matched layers (PML) at the truncated boundaries and the wide angle Padé approach.

unclear and cumbersome the introduction of proper radiation boundary conditions and wideangle features. Here, the vector operators are manipulated and presented in such a way that after only one (well acceptable) simplification, both PML and Padé approximants are straightforwardly introduced.

## 1. INTRODUCTION

Over the last decade, a considerable effort has been done to simulate in an efficient and accurate manner the electromagnetic propagation along optical waveguides. One of the most powerful numerical tools used in this field is the beam propagation method (BPM). Among the numerical methods available to discretize the waveguides' cross section, it is quite well established by now the superior performance achieved when the finite-element method is adopted. So far, a number of scalar, semivectorial and vectorial finite-element (FE) BPM schemes have been reported in the literature [1]-[3]. For dielectric media, it is quite clear that high accuracy and flexibility is attained by choosing the magnetic field as the wave equation's unknown, due to its continuity over the dielectric interfaces. This permits the use of nodal elements, which exhibit simpler expressions than the edge ones, specially for high order. For this situation, spurious solutions can be efficiently suppressed by forcing the divergence condition into the formulation, which will allow us, as additional advantage, to eliminate the axial field component. As a consequence, a highly efficient scheme, which solves the magnetic field's transverse components, is obtained. All this has been widely and thoroughly reported in the literature, specially in connection with the so called modal (eigenvalue) analysis [4]-[5]. For the BPM situation, such approach has been exploited by Obayya *et al.* [3] and Pinheiro *et al.* [6]. In the former isotropic media was considered, including PML and the wide-angle Padé approach; while in the latter, transverse anisotropy was treated, however, hard boundary conditions (perfect electric or magnetic walls) and paraxial propagation were adopted. The limitations exhibited in [6] are mainly due to the simplifications introduced in that formulation, making

## 2. FORMULATION

Starting from Maxwell equations, the double curl Helmholtz equation for the magnetic field,  $\vec{H}$ , is readily obtained,

$$\nabla \times (\bar{k} \nabla \times \vec{H}) - k_0^2 \vec{H} = 0 \quad (1)$$

where  $\bar{k} = 1/\bar{\epsilon}$ ,  $\bar{\epsilon}$  being the relative permittivity tensor. Considering dielectric media with transverse anisotropy, and defining the unit vectors  $\hat{u}_x$ ,  $\hat{u}_y$ , and  $\hat{u}_z$  associated with  $x$ ,  $y$ , and  $z$  directions, respectively,  $\bar{\epsilon}$  writes as follows,  $\bar{\epsilon} = \bar{\epsilon}_T + \epsilon_{zz} \hat{u}_z \hat{u}_z$ , where,  $\bar{\epsilon}_T$  is an arbitrary transverse tensor given by  $\bar{\epsilon}_T = \epsilon_{xx} \hat{u}_x \hat{u}_x + \epsilon_{xy} \hat{u}_x \hat{u}_y + \epsilon_{yx} \hat{u}_y \hat{u}_x + \epsilon_{yy} \hat{u}_y \hat{u}_y$ . Consequently,

$$\bar{k} = \bar{k}_T + k_{zz} \hat{u}_z \hat{u}_z \quad (2)$$

$$\bar{k}_T = \begin{bmatrix} k_{xx} & k_{xy} \\ k_{yx} & k_{yy} \end{bmatrix} = \bar{\epsilon}_T^{-1} \quad (3)$$

$$k_{zz} = \epsilon_{zz}^{-1} \quad (4)$$

In addition,  $k_0$  is the free space wavenumber and the operator  $\nabla$  is defined as,

$$\nabla = \hat{u}_x \mathbf{a}_x \frac{\partial}{\partial x} + \hat{u}_y \mathbf{a}_y \frac{\partial}{\partial y} + \hat{u}_z \mathbf{a}_z \frac{\partial}{\partial z} = \nabla_T + \hat{u}_z \mathbf{a}_z \frac{\partial}{\partial z} \quad (5)$$

where,  $\mathbf{a}_x$ ,  $\mathbf{a}_y$ , and  $\mathbf{a}_z$ , are parameters linked to the PML or virtual lossy media. Since the waves are assumed to

propagate along the  $z$  direction, the parameter  $\mathbf{a}_z$  is set to unity, while the other PML parameters have to be the inner computational domain and the PML. This ensures perfect wave matching over such interfaces, allowing the undesired radiation to leave the effective computational domain freely without any reflection. Following [7] and [8] the PML parameters are specified from the parameter  $S$  given below,

$$S = 1 - j \frac{3c}{2\omega_0 n d} \left( \frac{\mathbf{r}}{d} \right)^2 \ln \left( \frac{1}{R} \right) \quad (6)$$

where  $\omega_0$  is the angular frequency,  $d$  is the thickness of the PML,  $n$  is refractive index of the adjacent medium,  $\mathbf{r}$  is the distance from inner PML's interface and  $R$  is the reflection coefficient. Table I describes the parameters  $\mathbf{a}_x$  and  $\mathbf{a}_y$ .

TABLE I  
VALUES OF  $\mathbf{a}_x$  AND  $\mathbf{a}_y$

$\mathbf{a}_x$	$\mathbf{a}_y$	PML's location
$S$	$1$	Normal to $x$ direction
$1$	$S$	Normal to $y$ direction
$S$	$S$	On a corner

For regions outside the PML, i. e. inside the inner or effective computational domain, the parameters  $\mathbf{a}_{x,y}$  are set to unity. Next, the magnetic field's rapid variation is removed by writing,  $\vec{H}(x, y, z) = \vec{h}(x, y, z)e^{-jk_0 n_0 z}$ , where  $n_0$  is the reference effective index and  $\vec{h}(x, y, z) = \vec{h}_T(x, y, z) + \vec{h}_z(x, y, z)$  is the magnetic field's envelope or slow variation portion. Here,  $\vec{h}_T = h_x \hat{u}_x + h_y \hat{u}_y$  and  $\vec{h}_z = h_z \hat{u}_z$  represent the magnetic fields' (slow) transverse and axial components, respectively. Using in addition, the magnetic field divergence condition,  $\nabla \cdot \vec{H} = 0$ , which produces  $h_z = (\nabla_T \cdot \vec{h}_T + \partial h_z / \partial z) / \mathbf{g}$ , where,  $\mathbf{g} = jk_0 n_0$ , after some algebraic manipulations, the axial field can be effectively eliminated from (1), obtaining the following vectorial wave equation, in terms of the (slow) transverse component,

$$\begin{aligned} & \bar{k}_a \frac{\partial^2 \vec{h}_T}{\partial z^2} - (2\mathbf{g} \bar{k}_a - \mathbf{g}^{-1} \frac{\partial \bar{k}_a}{\partial z}) \frac{\partial \vec{h}_T}{\partial z} \\ & - \bar{k}_b \nabla_T (\nabla_T \cdot \vec{h}_T) - \nabla_T \times k_{zz} \nabla_T \times \vec{h}_T + \\ & \left( \bar{k}_c + \mathbf{g}^2 \bar{k}_a \right) \vec{h}_T = 0 \end{aligned} \quad (7)$$

The transverse tensors in (7) are defined below,

determined in such a way that the wave impedance be continuous across the interfaces formed between

$$\bar{k}_a = \begin{bmatrix} k_{yy} & -k_{yx} \\ -k_{xy} & k_{xx} \end{bmatrix} \quad (8)$$

$$\bar{k}_b = \mathbf{g}^{-1} \frac{\partial \bar{k}_a}{\partial z} - \bar{k}_a \quad (9)$$

$$\bar{k}_c = k_0^2 - \mathbf{g}^{-1} \frac{\partial \bar{k}_a}{\partial z} \quad (10)$$

where  $(\cdot)^\delta$ , denotes the transpose operation. By assuming that

$$\left| \mathbf{g}^{-1} \frac{\partial \bar{k}_a}{\partial z} \right| \ll \left| 2\mathbf{g} \bar{k}_a \right| \quad (11)$$

in the second term of (7), which is reasonable in most situations. Taking into account this approximation, which is the only one introduced in the present formulation, (7) becomes,

$$\begin{aligned} & \bar{k}_a \frac{\partial^2 \vec{h}_T}{\partial z^2} - 2\mathbf{g} \bar{k}_a \frac{\partial \vec{h}_T}{\partial z} \\ & - \bar{k}_b \nabla_T (\nabla_T \cdot \vec{h}_T) - \nabla_T \times k_{zz} \nabla_T \times \vec{h}_T + \\ & \left( \bar{k}_c + \mathbf{g}^2 \bar{k}_a \right) \vec{h}_T = 0 \end{aligned} \quad (12)$$

Comparing (12) with the expression (1) in [6], becomes evident the improvement achieved here, not only in clearness and neatness, but also in accuracy, since expression (1) in [6] was obtained at the expense of two approximations instead of one. Next, applying the conventional finite element method to the transverse variation of (12), the cross sectional domain  $\mathbf{W}$ , is divided in  $N_{el}$  triangles, producing  $N_p$  unknowns over the corresponding nodes. Introducing a set of basis functions (Lagrangian polynomials of first or second order),  $\{\phi_j\}$ ,  $j=1, \dots, N_p$ ;  $\vec{h}_T(x, y, z)$  is expressed as follows,

$$\vec{h}_T(x, y, z) = \sum_{j=1}^{N_{px}} h_{xj}(z) \mathbf{y}_j(x, y) \hat{u}_x + \sum_{j=N_{px}+1}^{N_p} h_{yj}(z) \mathbf{y}_j(x, y) \hat{u}_y \quad (13)$$

where the coefficients  $h_{xj}$  and  $h_{yj}$  represent the unknown field values on the partition's nodes. This expansion, which defines the so-called FE discretization process, leads to the matrix problem given below,

$$[M] \frac{\partial^2 \{\bar{h}_T\}}{\partial z^2} - 2\mathbf{g}[M] \frac{\partial \{\bar{h}_T\}}{\partial z} + ([K] + \mathbf{g}^2 [M]) \{\bar{h}_T\} = \{0\} \quad (14)$$

Where  $\{\bar{h}_T\}$  represents a column vector containing the unknowns  $h_{xj}$  and  $h_{yj}$ ,  $\{0\}$  is the null column vector, and  $[M]$  and  $[K]$  are the so-called global matrices, defined by

$$[M]_{ij} = \int_{\Omega} \bar{k}_a \bar{y}_j \cdot \bar{y}_i d\Omega \quad (15)$$

$$[K]_{ij} = - \int_{\Omega} (k_{zz} \nabla_T \times \bar{y}_j) \cdot (\nabla_T \times \bar{y}_i) d\Omega + \int_{\Omega} (\nabla_T \times \bar{y}_j) \nabla_T \cdot (\bar{k}_b \bar{y}_i) d\Omega - \oint_{\partial\Omega} (\nabla_T \cdot \bar{y}_j) (\bar{k}_b \bar{y}_i) \cdot \hat{n} dl + \int_{\Omega} \bar{k}_c \bar{y}_j \cdot \bar{y}_i d\Omega \quad (16)$$

here,

$$\bar{y}_j = \mathbf{y}_j \hat{u} \quad (17)$$

$$\hat{u} = \hat{u}_x \quad \text{for } j=1, \dots, Npx \quad (18)$$

$$\hat{u} = \hat{u}_y \quad \text{for } j=Npx+1, \dots, Np \quad (19)$$

In (16),  $\partial\Omega$  represents all boundaries over the cross sectional domain  $\Omega$ , and  $\hat{n}$ , the outward normal unit vector linked to those boundaries. Namely,  $\mathcal{I}\Omega$  includes all interfaces ( $\mathcal{I}\Omega_{interf}$ ) and the external boundary ( $\mathcal{I}\Omega_{ext}$ ). The latter corresponds to the truncated boundary, assumed here to be of rectangular shape, which separates the PML and the infinitely extended region. Since all radiation is supposed to be absorbed inside the PML,  $\partial\Omega_{ext}$  can be chosen to be a PEC (Perfect Electric Conductor) or PMC (Perfect Magnetic Conductor). Here, we choose the former. As observed in previous publications [4], [5], the line integral in (16) vanishes over PEC walls, but not over interfaces, where the media exhibits step discontinuity. Therefore, here, such line integral needs to be computed only over  $\partial\Omega_{interf}$ . Matrices  $[M]$  and  $[K]$  can also be expressed as a summation of element matrices linked to the  $x$  and  $y$  coordinates, over all elements  $e$ . Following [8], the Padé (1,1) approximation [9], can be straightforwardly applied to (14), producing the matrix equation given below,

$$[\tilde{M}] \frac{d\{\bar{h}_T\}}{dz} + [K] \{\bar{h}_T\} = \{0\} \quad (20)$$

with,

$$[\tilde{M}] = [M] - \frac{1}{4g^2} ([K] + \mathbf{g}^2 [M]) \quad (21)$$

Finally, the  $\mathbf{q}$  - finite difference marching scheme, applied to (36), writes as follows,

$$\begin{aligned} &([\tilde{M}(z)] + \mathbf{q}\Delta z [K(z)]) \{\bar{h}_T(z + \Delta z)\} = \\ &([\tilde{M}(z)] - (1 - \mathbf{q})\Delta z [K(z)]) \{\bar{h}_T(z)\} \end{aligned} \quad (22)$$

where,  $\Delta z$  is the step's size along the propagation coordinate, and  $\mathbf{q}$  ( $0 \leq \mathbf{q} \leq 1$ ) is introduced to control the stability of the method. Extensive tests have shown that stability is ensured when  $0.5 \leq \mathbf{q} \leq 1$ . All results presented here were simulated with  $\mathbf{q} = 0.55$ .

### 3. RESULTS

To validate our numerical technique we first considered an anisotropic planar waveguide with transverse dimensions  $a$ ,  $b$  as shown in Fig. 1.,  $a = b = 1\mu\text{m}$ . The channel is embedded in an isotropic dielectric media with index equal to  $\sqrt{2.05}$ , surrounded by a PML with thickness  $d = 1.0 \mu\text{m}$ . The channel's ordinary and extraordinary refractive indexes are  $\sqrt{2.19}$  and  $\sqrt{2.31}$  [11], respectively.

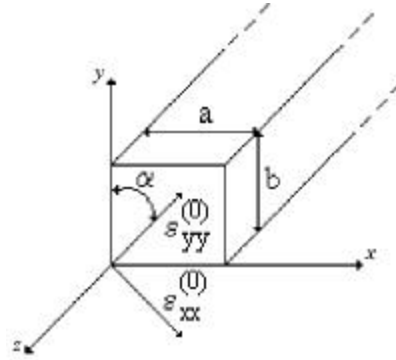


Fig. 1. Anisotropic waveguide optical axes exhibiting an angular displacement  $\mathbf{a}$

Here  $\epsilon_{xx}^{(0)}$ ,  $\epsilon_{yy}^{(0)}$  and  $\epsilon_{zz}^{(0)}$  are the terms of the diagonal tensor  $\epsilon$  when the optical axes are aligned with coordinates  $x$  and  $y$ . In this simulation we considered a computational window of  $8 \mu\text{m}$  ( $x$ -direction)  $\times$   $8 \mu\text{m}$  ( $y$ -direction) covered by 3814 linear elements, while in [11] was used a computational window of  $34 \mu\text{m} \times 34 \mu\text{m}$  covered by 4784 linear elements, the wavelength was  $\lambda = 0.86 \mu\text{m}$  and  $\mathbf{a} = 45^\circ$ . The permittivity tensor terms are, [12]:

$$\mathbf{e}_{xx} = n_o^2 \cos^2 \mathbf{a} + n_e^2 \sin^2 \mathbf{a} \quad (23)$$

$$\mathbf{e}_{yy} = n_e^2 \cos^2 \mathbf{a} + n_o^2 \sin^2 \mathbf{a} \quad (24)$$

$$\mathbf{e}_{zz} = n_o^2 \quad (25)$$

$$\mathbf{e}_{xy} = \mathbf{e}_{yx} = (n_e^2 - n_o^2) \cos \mathbf{a} \sin \mathbf{a} \quad (26)$$

where  $\mathbf{a}$  is the rotation angle of the main tensor axes related to the  $x$  and  $y$  coordinates. The waveguide was excited at  $z = 0$  with the fundamental quasi TM mode  $E_{11}^x$ , with  $\mathbf{a}=0$ , and its corresponding effective propagation constant ( $\mathbf{b} / k_0$ ), obtained using a modal eigenvalue method [5]. Fig. 2 shows the normalized intensity variations of  $h_x$  and  $h_y$  components for a propagation step of  $\Delta z = 0.1 \mu\text{m}$ . The switching to a quasi TE beam occurred at  $z = 17 \mu\text{m}$ , showing perfect agreement with [11].

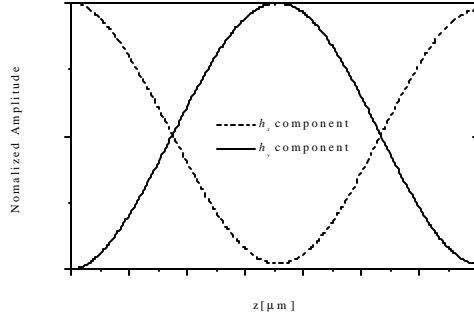


Fig. 2. Variation of  $h_x$ 's and  $h_y$ 's normalized amplitudes along  $z$  direction.

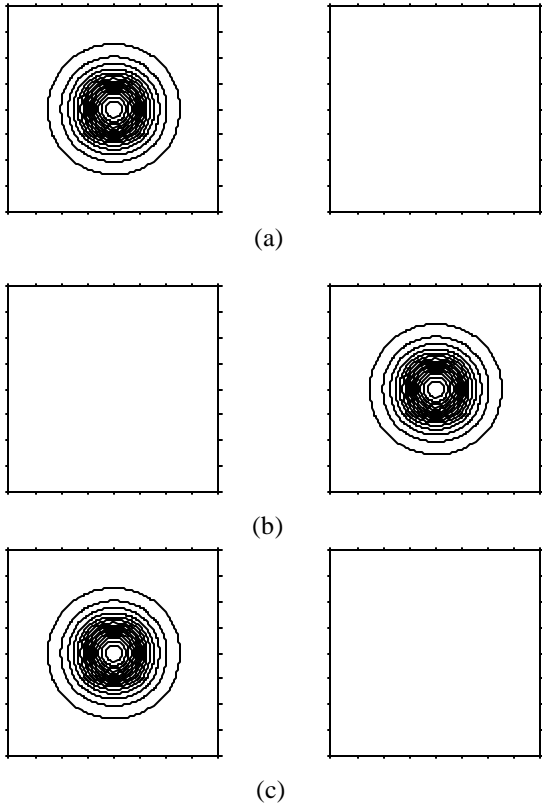


Fig. 3. Modulus of  $h_x$  (left column) and modulus of  $h_y$  (right column), at (a)  $z = 0 \mu\text{m}$ , (b)  $z = 18 \mu\text{m}$ , (c)  $z = 35 \mu\text{m}$ .

As we can see in Fig. 2 and Fig. 3, the field resumes its initial configuration again at  $z = 35 \mu\text{m}$ , which is in agreement with the value obtained through the relation

$L_B = \frac{\lambda}{|\mathbf{b}_{eff1} - \mathbf{b}_{eff2}|}$  [12], where  $L_B$  is the beating length and  $\mathbf{b}_{eff1}$  and  $\mathbf{b}_{eff2}$  are the effective propagation constants of the modes  $E_{11}^x$  and  $E_{11}^y$ , respectively. Through modal analysis [5] we found  $\mathbf{b}_{eff1} = 1.47393494$  and  $\mathbf{b}_{eff2} = 1.44930071$ , therefore, the beating length was  $34.9107670 \mu\text{m}$ , which is in good agreement with the value obtained by the present BPM.

Next, we consider an anisotropic optical waveguide whose cross-section and numerical window are illustrated in Fig. 4, [13]. The substrate is made of  $\text{LiNbO}_3$  (LN), the guiding region is made of proton-exchanged  $\text{LiNbO}_3$  (PE-LN). The waveguide thickness and the width are, respectively,  $t = 2 \text{ mm}$  and  $w = 2 \text{ mm}$ . The substrate has ordinary and extraordinary indexes are, respectively,  $n_o = 2.250$  and  $n_e = 2.172$ , and the refractive index difference between the guiding region and the substrate is  $\Delta n_e = 0.02$  for the extraordinary index. The component of the symmetric relative permittivity tensor for the substrate are given by (23)-(26). As input, a horizontally ( $\hat{x}$ ) polarized Gaussian beam was considered. The wavelength was  $\lambda = 0.84 \text{ mm}$  and the beam spot size was  $0.6 \text{ mm}$ . The computational window was  $8 \text{ mm}$  ( $x$ -direction)  $\times$   $6 \text{ mm}$  ( $y$ -direction), and was surrounded by PML with thickness  $d = 2 \text{ mm}$ . Fig. 5 shows the variation of  $h_x$ 's and  $h_y$ 's modulus, along the propagation coordinate, with  $\mathbf{a} = 45^\circ$  and propagation step,  $\Delta z = 0.1 \text{ mm}$ . The input beam's expected transformation into the fundamental mode, is clearly observed in Fig. 5. Reflections from the computational windows are not perceptible, which demonstrates the PML's efficiency. After  $400 \text{ mm}$ , the fundamental mode is completely well established. The variation of  $h_y$ 's modulus from zero until it equals the  $h_x$ 's modulus, is neatly shown in Fig. 5. This behavior is consistent with the hybrid characteristic of the fundamental mode, and is in perfect agreement with the results reported in [13].

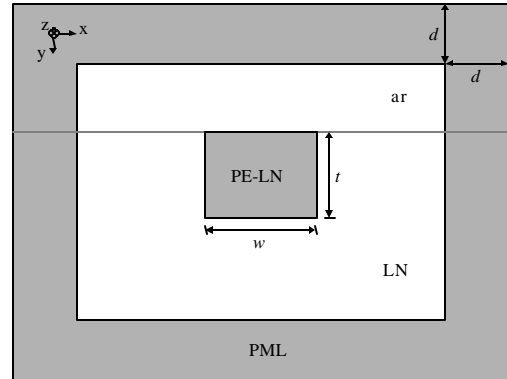


Fig. 4. Anisotropic optical waveguide's cross-section and numerical window surrounded by PML.

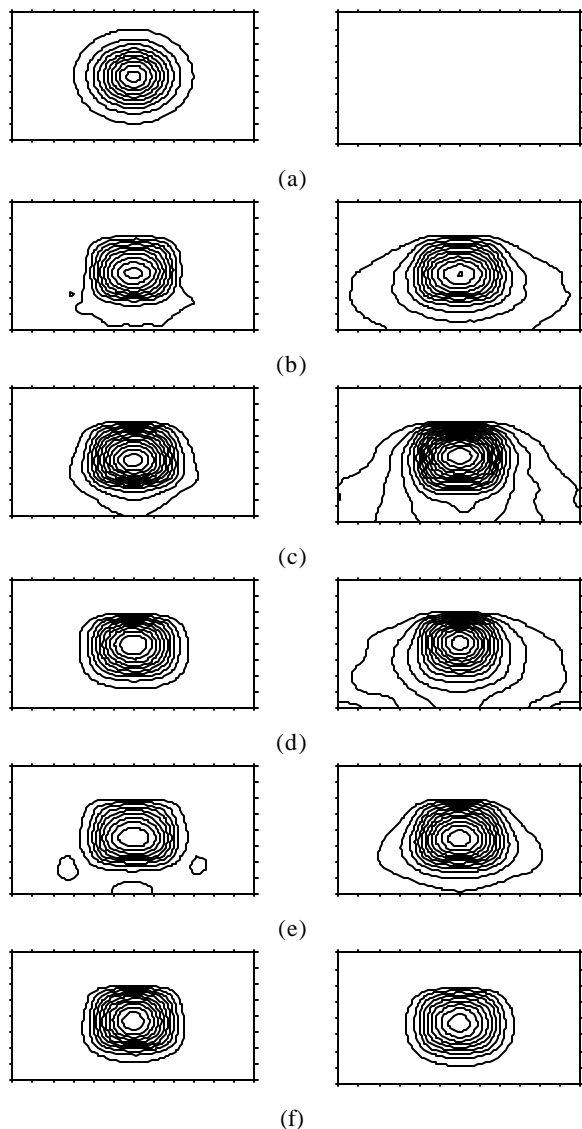


Fig. 5. Modulus of  $h_x$  (left column) and modulus of  $h_y$  (right column), at (a)  $z = 0$  mm, (b)  $z = 20$  mm, (c)  $z = 40$  mm, (d)  $z = 60$  mm, (e)  $z = 80$  mm e (f)  $z = 500$  mm

#### 4. SUMMARY

A vectorial finite-element BPM for transverse anisotropic media, was presented in detail, which constitutes a substantial improvement on the scheme published in [6]. The present improved scheme is based on a practically new formulation, which permits the insertion of PML conditions and wide-angle approximations, in a neat and straightforward manner. Its efficiency and usefulness was demonstrated through the analysis of two key examples.

#### 5. REFERENCES

[1] Y. Tsuji, M. Koshiba and N. Takimoto, "Finite element beam propagation method for anisotropic optical

waveguides", *Journal Lightwave Technology*, Vol. 17, No. 4, pp.723-828, April 1999.

[2] P. Liu and B. J. Li, "Semivectorial beam-propagation method for analyzing polarized modes of rib waveguide", *IEEE J.Quantum Electron*, Vol. 28, pp. 778-782, April 1992.

[3] S. S. A. Obayya, B. M. A. Rahman and H. A. El-Mikati, "New-vectorial numerically efficient propagation algorithm based on the finite element method", *IEEE Journal Lightwave Technology*, Vol. 18, No. 3, pp. 409-415, March 2000.

[4] Y. L. Lu and F. A. Fernández, "An efficient finite-element solution for inhomogeneous anisotropic and lossy dielectric waveguides", *IEEE Trans. on Microwave Theory and Techniques*, Vol. 41, Nos. 6-7, pp. 1215-1223, June-July 1993.

[5] H. E. Hernández-Figueroa, F. A. Fernández, Y. Lu and J. B. Davies, "Vectorial finite element modeling of 2D leaky waveguides", *IEEE Trans. Magn.*, Vol. 33, No. 4, pp.1710-1713, May 1995.

[6] H. F. Pinheiro and H. E. Hernández-Figueroa, "Novel finite-flement formulation for vectorial Beam Propagation Analysis in anisotropic medium", *IEEE Photonics Technology Letters*, Vol. 12, No. 2, pp. 155-157, February 2000.

[7] J. P. Berenger, "A perfectly matched layer for the absorption of electromagnetic waves", *J. Compt. Phys.*, Vol. 114, No. 10, pp. 185-200, October 1994.

[8] M. Koshiba, Y. Tsuji and M. Hikari, "Finite-element beam-propagation method with perfectly matched layers boundary conditions", *IEEE Transactions on Magnetics*, Vol. 35, No. 3, pp. 1482-1485, May 1999.

[9] G. R. Hadley, "Wide-angle beam propagation using Padé approximation method", *Optics Letters*, Vol. 17, No. 10, pp. 1426-1428, October 1992.

[10] Y. Tsuji and M. Koshiba, "Adaptive mesh generation for full-vectorial guided-mode and beam-propagation solutions", *IEEE Journal of Selected Topics in Quantum Electronics*, Vol. 6, No 1, pp. 163-169, January/February 2000.

[11] H. F. Pinheiro, "Vectorial beam propagation method based on finite-elements", Ph D Thesis (in Portuguese), UNICAMP, Brazil, February 2000.

[12] H. E. Hernández-Figueroa, "Simple nonparaxial beam propagation scheme for integrated optics", *IEEE Journal Lightwave Technology*, Vol. 12, No. 4, pp.644-649, April 1994.

[13] K. Saitoh and M. Koshiba, "Approximate scalar finite-element beam-propagation method with perfectly matched layers for anisotropic optical waveguides", *IEEE Journal of Lightwave and Technology*, Vol. 19, No. 5, pp. 786-792, May 2001.